

A Correlation Based Double Directional Stochastic Model for MIMO-UWB Propagation Channels

Xuemin Hong and Chengxiang Wang
 Heriot-Watt University
 School of Engineering & Physical Sciences
 Electrical, Electronic and Computer Engineering,
 Edinburgh EH14 4AS, UK
 E-mail: xh12@hw.ac.uk, cheng-xiang.wang@hw.ac.uk

Keywords— UWB, MIMO, channel model, spatial correlation

Abstract— This paper proposes a correlation based double directional stochastic model (CBDDSM) for indoor Multiple Input Multiple Output (MIMO) Ultra Wideband (UWB) propagation channels in the passband domain. Both angle of arrival (AoA) and time of arrival statistics are taken into account in the modelling procedure. Spatial correlations are introduced into the amplitude matrices and delay matrices of the channel model. Under the assumption of Rayleigh amplitude fading statistics, each amplitude matrix is obtained from the underlying correlated complex Gaussian matrix, while each delay matrix is obtained as the sum of a reference matrix and a difference matrix. Model parameters are determined based on well-known measurement campaigns. Simulation results show that the characteristics of the proposed model are compatible with those of the IEEE 802.15.3a standard model. In addition, our initial analysis indicates that this model yields desirable spatial correlation properties in both the time and frequency domains.

I. INTRODUCTION

UWB and MIMO systems have attracted great research interests in the past few years due to their appealing features. Their combination leads to MIMO-UWB. MIMO-UWB systems have the potential to improve the system performance in many ways. Through spatial diversity combining, MIMO-UWB can provide more reliable radio link and wider radio range [1][2]. Through spatial multiplexing, MIMO-UWB can support very high data rate communications [3][4]. Other potential benefits of MIMO-UWB include interference cancellation [5] and immunity against timing jitter [6].

Channel characteristics are crucial for the design and performance evaluation of MIMO-UWB systems. The widely used assumption of spatial uncorrelatedness will degenerate a MIMO-UWB channel into independent Single Input Single Output (SISO) channels [7]. However, such assumption leads to unrealistic over-estimations of the MIMO signaling performance in practical systems [8]. In the literature, there are only a few models addressing the spatial characteristics of UWB channels. For example, a space-variant UWB channel model was presented in [9][10]. This model can be classified as Geometrically Based Stochastic Models (GBSMs), which have implicit spatial correlations. Consequently, this model is difficult to be integrated into theoretical frameworks and therefore provide few insights into the signaling design over

MIMO-UWB systems. From the information theory and signal processing perspectives, a new channel model is thus desirable to address the spatial correlation characteristics explicitly.

The objective of this paper is to provide a MIMO-UWB channel model which can yield explicit and concise analytical expressions for its spatial correlation characteristics. Inspired by baseband Correlation Based Stochastic Models (CBSMs) [11], we propose a correlation based passband channel model for MIMO-UWB. In this model, the spatial correlations for path amplitudes and path delays are defined separately and explicitly.

The rest of the paper is organized as follows. A double directional SISO-UWB spatial channel model is introduced in Section II. Section III proposes a correlation based double directional MIMO-UWB channel model. Section IV describes an example implementation and evaluates the proposed model based on simulation results. Finally, conclusions are drawn in Section V. Note that for simplicity, the term “correlation” refers to “spatial correlation” in the rest of the paper.

II. DOUBLE-DIRECTIONAL SISO-UWB CHANNEL MODEL

As a natural combination of the S-V model [12] and the double directional model [13], a double directional SISO UWB channel model gives the channel impulse response by:

$$h(t) = X \sum_l \sum_k a_{k,l} \delta(t - T_l - \tau_{k,l}) \times \delta(\varphi_T - \varphi_{k,l,AoD}) \delta(\varphi_R - \varphi_{k,l,AoA}) \quad (1)$$

where X represents the log-normal shadowing, $a_{k,l}$ is the multipath gain coefficient for the k th ray of the l th cluster, T_l is the arrival time of the first ray of the l th cluster, $\tau_{k,l}$ is the delay of the k th ray of the l th cluster relative to the first path arrival time T_l , $\varphi_{k,l,AoA}$ and $\varphi_{k,l,AoD}$ are the AoA and Angle of Departure (AoD) for the corresponding ray, respectively. From Fig. 1, $\varphi_{k,l,AoA}$ and $\varphi_{k,l,AoD}$ are given by:

$$\varphi_{k,l,AoA} = \theta_R + \delta_{l,AoA} + \phi_{k,l,AoA} \quad (2)$$

$$\varphi_{k,l,AoD} = \theta_T + \delta_{l,AoD} + \phi_{k,l,AoD} \quad (3)$$

respectively. Here, θ_R and θ_T are the angles between the Tx-Rx Line of Sight (LOS) and the broadside of Rx and Tx, respectively, $\delta_{l,AoA}$ and $\delta_{l,AoD}$ are the AoA and AoD for the

l th cluster with respect to θ_R and θ_T , respectively, $\phi_{k,l,AoA}$ and $\phi_{k,l,AoD}$ are the offset angles for the k th ray of the l th cluster with respect to $\delta_{l,AoA}$ and $\delta_{l,AoD}$, respectively.

III. MIMO-UWB CHANNEL MODELLING

Fig. 2 shows a double-directional MIMO link with Uniform Linear Arrays (ULA) at both the Tx and Rx. The channel impulse response matrix in the passband domain for the k th ray of the l th cluster is given by

$$\mathbf{H}_{k,l} = \begin{bmatrix} h_{1,1}^{k,l} & \cdots & h_{1,n_R}^{k,l} \\ \vdots & h_{i,j}^{k,l} & \vdots \\ h_{n_T,1}^{k,l} & \cdots & h_{n_T,n_R}^{k,l} \end{bmatrix} \quad (4)$$

where $h_{i,j}^{k,l}$ denotes the double directional channel impulse response from the i th Tx to the j th Rx, for the k th ray of the l th cluster. It is a function of the ray amplitude, delay (arrival time), AoA and AoD, i.e., $h_{i,j}^{k,l} = F(a_{i,j}^{k,l}, \epsilon_{i,j}^{k,l}, \varphi_{AoA,i,j}^{k,l}, \varphi_{AoD,i,j}^{k,l})$. Here, $a_{i,j}^{k,l}$ denotes the ray amplitude, $\epsilon_{i,j}^{k,l}$ denotes the ray arrival time and is given by

$$\epsilon_{i,j}^{k,l} = T_{i,j}^l + \tau_{i,j}^{k,l} \quad (5)$$

where $T_{i,j}^l$ denotes the l th cluster arrival time (defined as the arrival time for the first ray within the cluster), and $\tau_{i,j}^{k,l}$ denotes the k th intra-cluster ray arrival time with respect to $T_{i,j}^l$, $\varphi_{AoA,i,j}^{k,l}$ and $\varphi_{AoD,i,j}^{k,l}$ denote the AoA and AoD for each ray, respectively. Under the plane wave and small antenna array assumptions, $\varphi_{AoA,i,j}^{k,l}$ and $\varphi_{AoD,i,j}^{k,l}$ degenerate to $\varphi_{AoA}^{k,l}$ and $\varphi_{AoD}^{k,l}$, respectively. It is important to mention that the delay parameters $\epsilon_{i,j}^{k,l}$ are assumed to be independent from the angle parameters $\varphi_{AoA}^{k,l}$ and $\varphi_{AoD}^{k,l}$.

Since the following discussions will be the same for each ray, the index k and l are dropped for simplification. As long as the passband channel modelling is considered and omni-directional antennas are applied, we can focus on the amplitude matrix \mathbf{A} and the delay matrix $\mathbf{\Pi}$ given by

$$\mathbf{A} = \begin{bmatrix} a_{1,1} & \cdots & a_{1,n_R} \\ \vdots & a_{i,j} & \vdots \\ a_{n_T,1} & \cdots & a_{n_T,n_R} \end{bmatrix} \quad (6)$$

$$\mathbf{\Pi} = \begin{bmatrix} \epsilon_{1,1} & \cdots & \epsilon_{1,n_R} \\ \vdots & \epsilon_{i,j} & \vdots \\ \epsilon_{n_T,1} & \cdots & \epsilon_{n_T,n_R} \end{bmatrix}. \quad (7)$$

In the following, methods of generating spatially correlated \mathbf{A} and $\mathbf{\Pi}$ will be introduced. Correlation matrices will be defined explicitly for both \mathbf{A} and $\mathbf{\Pi}$. The connections between \mathbf{A} and $\mathbf{\Pi}$ will also be addressed.

A. Spatially Correlated Amplitude Matrix \mathbf{A}

First of all, we assume that the amplitudes $|a_{i,j}|$ follow Rayleigh distributions. This assumption is supported by measurement campaigns reported in [14][15], and is considered to be valid in the following cases: (i) a dense multipath

environment (e.g., an industrial environment) with a system bandwidth as high as 7.5GHz [14]; (ii) a home/office environment with a smaller system bandwidth (e.g., multi-band applications) [15]. In such cases, each resolvable ray is still the superposition of many irresolvable sub-rays. Therefore, the underlying baseband channel coefficients $g_{i,j}$ can be treated as complex Gaussian random variables. Then we have $a_{i,j} = p|g_{i,j}|$, where p takes the value of equiprobable ± 1 to account for signal inversion due to reflections. Therefore, \mathbf{A} can be fully characterized by the underlying baseband channel matrix \mathbf{G} . In other words, spatially correlated matrix \mathbf{A} can be obtained from spatially correlated matrix \mathbf{G} .

Assuming φ_{AoA} and φ_{AoD} to be independent, the MIMO channel correlation matrix \mathbf{R} is given as the Kronecker product of the transmit antenna correlation matrix \mathbf{R}_T and the receive antenna correlation matrix \mathbf{R}_R [16]:

$$\mathbf{R} = \text{vec}(\mathbf{G})^H \text{vec}(\mathbf{G}) = \mathbf{R}_T \otimes \mathbf{R}_R \quad (8)$$

where \otimes denotes the Kronecker product, $(\cdot)^H$ is the conjugate transpose and $\text{vec}(\cdot)$ operator rearranges the $n_T \times n_R$ matrix \mathbf{G} into a column vector of size $n_T n_R \times 1$. According to [16], matrices \mathbf{R}_T and \mathbf{R}_R can be calculated as functions of φ_{AoD} and φ_{AoA} , respectively. Given \mathbf{R} , correlated \mathbf{G} can be obtained from independent Gaussian random variables by [17]:

$$\text{vec}(\mathbf{G}) = \mathbf{C}\mathbf{U} \quad (9)$$

where \mathbf{C} is the standard Cholesky factorization of the matrix $\mathbf{R} = \mathbf{C}\mathbf{C}^T$ provided that \mathbf{R} is nonsingular. \mathbf{U} is a $n_T n_R \times 1$ vector whose entries μ_n ($n = 1, \dots, n_T n_R$) are zero-mean independent identically distributed (i.i.d.) complex Gaussian random variables with identical variance of σ . One can easily derive that each row of the matrix \mathbf{C} fulfills:

$$\sum_{p=1}^{n_T n_R} c_{p,q}^2 = 1, \quad q = 1, \dots, n_T n_R \quad (10)$$

where p and q are the indices for row and column, respectively. From (9) and (10), it is obvious that $g_{i,j}$ also have identical variances of σ .

B. Spatially Correlated Delay Matrix $\mathbf{\Pi}$

As shown in Fig. 2, an incoming ray reaches different receive antennas with different delays. We define such delay differences as the Inter-Antenna Propagation delay Difference (IAPD). Under the plane wave assumption, the IAPD between the j_1 th and j_2 th receive antennas is given by:

$$\Delta\mu_{j_1,j_2}^R = \frac{d_{j_1,j_2} \sin(\varphi_{AoA})}{c} \quad (11)$$

where d_{j_1,j_2} is the distance between two antennas, φ_{AoA} is the AoA of the incoming ray and c is the speed of light. Without loss of generality, we chose $j = 1$ as the reference antenna and construct the delay difference vector $\Delta\tilde{\mu}_R$ as:

$$\Delta\tilde{\mu}_R = (0, \dots, \Delta\mu_{j_1,j_2}^R, \dots, \Delta\mu_{1,n_R}^R)^T. \quad (12)$$

Similarly, a delay difference vector $\Delta\tilde{\mu}_T$ can be defined for the transmit antenna array.

From Fig. 2, we further assume that the Inter-Channel Propagation delay Difference (ICPD) is the sum of the transmit IAPD and receive IAPD, i.e.,

$$\epsilon_{i1,j1} - \epsilon_{i2,j2} = \Delta\mu_{i1,i2}^T + \Delta\mu_{j1,j2}^R. \quad (13)$$

We then write the delay matrix $\mathbf{\Pi}$ as the sum of a reference matrix and a difference matrix :

$$\mathbf{\Pi} = \mathbf{\Pi}_r + \Delta\mathbf{\Pi}_r \quad (14)$$

where the reference matrix $\mathbf{\Pi}_r$ is a $n_T \times n_R$ matrix with identical entries of the reference delay ϵ_r . Without loss of generality, we set $\epsilon_r = \epsilon_{1,1}$. The difference matrix $\Delta\mathbf{\Pi}_r$ with respect to the chosen reference matrix is therefore given by:

$$\Delta\mathbf{\Pi}_r = \begin{bmatrix} 0 & \cdots & \Delta\mu_{1,n_R}^R \\ \vdots & \Delta\mu_{1,i}^T + \Delta\mu_{1,j}^R & \vdots \\ \Delta\mu_{1,n_T}^T & \cdots & \Delta\mu_{1,n_T}^T + \Delta\mu_{1,n_R}^R \end{bmatrix}. \quad (15)$$

$\Delta\mathbf{\Pi}_r$ gives the insight of the correlation between antenna spatial positions and channel delays. Thus it can be regarded as the ‘‘correlation matrix’’ in the delay domain. Note that $\Delta\mathbf{\Pi}_r$ can be calculated from $\Delta\tilde{\mu}_T$ and $\Delta\tilde{\mu}_R$ by:

$$\Delta\mathbf{\Pi}_r = \Delta\tilde{\mu}_T \oplus (\Delta\tilde{\mu}_R)^T \quad (16)$$

where \oplus denotes the alternative matrix addition [18], which is defined analogous to matrix multiplication, e.g.,

$$\begin{bmatrix} a \\ b \end{bmatrix} \oplus \begin{bmatrix} c & d \end{bmatrix} = \begin{bmatrix} a+c & a+d \\ b+c & b+d \end{bmatrix}. \quad (17)$$

C. Correlated \mathbf{A} and $\mathbf{\Pi}$

From here we restore the ray index k and cluster index l . Recalling (5), we write the reference delay for the k th ray of the l th cluster as:

$$\epsilon_r^{k,l} = T_r^{k,l} + \tau_r^{k,l} \quad (18)$$

where T_r^l and $\tau_r^{k,l}$ are the cluster arrival time and ray arrival time for the reference ray. According to [7], both T_r^l and $\tau_r^{k,l}$ are modelled as poisson processes given by [7]:

$$p(T_r^l | T_r^{l-1}) = \Lambda \exp[-\Lambda(T_r^l - T_r^{l-1})], \quad l > 0 \quad (19)$$

$$p(\tau_r^{k,l} | \tau_r^{k-1,l}) = \lambda \exp[-\lambda(\tau_r^{k,l} - \tau_r^{k-1,l})], \quad k > 0 \quad (20)$$

where Λ is the cluster arrival rate, and λ is the ray arrival rate.

Given matrix $\mathbf{A}^{k,l}$ and its underlying complex Gaussian random variable $\mu^{k,l}$, as well as matrix $\mathbf{\Pi}^{k,l}$ and its reference delay $\epsilon_r^{k,l} = T_r^l + \tau_r^{k,l}$, we follow the same exponential power decay in [7] and have:

$$\sigma_{k,l}^2 = E[|\mu_n^{k,l}|^2] = \Omega_0 \exp\left(\frac{-T_r^l}{\Gamma}\right) \exp\left(\frac{-\tau_r^{k,l}}{\gamma}\right) \quad (21)$$

where $\sigma_{k,l}^2$ is the energy of $\mu_n^{k,l}$, Γ is the cluster decay factor, γ is the ray decay factor, and Ω_0 is the mean energy of the first ray of the first cluster. Without shadowing, the total energy of an impulse response is normalized to be 1, i.e.,

$$\sum_l \sum_k \sigma_{k,l}^2 = 1. \quad (22)$$

IV. IMPLEMENTATION EXAMPLE AND EVALUATIONS

A. Parametrization and Implementation

In this example, all delay-related parameters are set to be the same as IEEE 802.15.3a Channel Model 2 (CM2), which is specified as a NLOS channel model in the range of 0 to 4 meters [7]. In addition, angle-related parameters are specified according to the measurement campaign reported in [19].

1) Initialization:

θ_R and θ_T are i.i.d., uniformly distributed from 0 to 360 degree. n_T , n_R , Tx spacing unit d_T and the Rx spacing unit d_R are specified by the user.

2) Calculate the Reference Parameters $\epsilon_r^{k,l}$ and $\sigma_{k,l}$:

Reference ray delay $\epsilon_r^{k,l}$ and the corresponding ray energy $\sigma_{k,l}$ is calculated according to (18)-(22).

3) Calculate the Angle Parameters $\varphi_{AoA}^{k,l}$ and $\varphi_{AoD}^{k,l}$:

$\varphi_{AoA}^{k,l}$ and $\varphi_{AoD}^{k,l}$ are independent, constructed according to (2) and (3). Both δ_{AoA}^l and δ_{AoD}^l are i.i.d., uniformly distributed from 0 to 360 degree [19]. Both $\phi_{AoA}^{k,l}$ and $\phi_{AoD}^{k,l}$ follow zero-mean Laplacian distribution with a standard deviation of 38 degree [19].

4) Calculate the Amplitude Matrix $\mathbf{A}^{k,l}$:

For each ray, given $\sigma_{k,l}$ from step 2, $\varphi_{AoA}^{k,l}$ and $\varphi_{AoD}^{k,l}$ from step 3, the amplitude matrix $\mathbf{A}^{k,l}$ is calculated according to (8) and (9). We refer to [16] for the calculations of \mathbf{R} . The Angle Spread (AS) of sub-rays are empirically chosen as 5 degree for both the Tx and Rx; f_c is set to be 6.85 GHz; the Power Azimuth Spectrum (PAS) shape for irresolvable sub-rays is assumed as uniform.

5) Calculate the Delay Matrix $\mathbf{\Pi}^{k,l}$:

For each ray, given $\epsilon_r^{k,l}$ from step 2, $\varphi_{AoA}^{k,l}$ and $\varphi_{AoD}^{k,l}$ from step 3, the delay matrix $\mathbf{\Pi}^{k,l}$ can be calculated according to (11) to (16).

6) Discretization:

The same discretization process is carried out as specified in [7]. The sampling interval T_s is specified by the user.

With $d_T=10$ cm, $d_R=20$ cm and $T_s=0.167$ ns, a typical realization of a 2×2 MIMO channel is shown in Fig. 3.

B. Evaluations and Discussions

We first show our model to be compatible with the IEEE 802.15.3a standard SISO model in terms of major channel characteristics. With $d_T=10$ cm, $d_R=20$ cm and $T_s=0.167$ ns, a 2×2 MIMO channel is realized 1000 times. Model characteristics are then extracted and compared with the CM2 targets in Table 1. Good agreements are observed in all cases, namely, the Mean Excess Delay (MED), the Mean RMS delay (MRMS) and the mean Number of significant Paths capturing $> 85\%$ energy (NP(85)). We recall that in our model, the small scale fading mechanism is assumed to be Rayleigh, which differs from Log-normal as proposed in CM2. The compatibility of our model actually suggests that small scale fading mechanisms might not have significant impacts on the major characteristics of a SISO UWB channel. The reason

could be that the power-delay decay law as described by (21) has dominant effects over small scale fading mechanisms. Figs. 4 and 5 aim to prove that the proposed model does not cause significant variances among individual SISO channels. Fig. 4 shows the Cumulative Distribution Function (CDF) of the channel excess delay while Fig. 5 shows the CDF of NP(85) for all four SISO channels in a 2×2 MIMO link. In both figures, the characteristics of all four SISO channels agree well. We note that good agreements are also observed for CDFs of channel RMS delay, channel energy and number of significant paths with 10 dB of peak.

Table. 1 CM2 targets and the characteristics of the proposed channel model (a 2×2 MIMO link)

	MED(ns)	MRMS(ns)	NP(85)
Target	10.38	8.03	36.1
T1R1	10.48	8.29	35.12
T1R2	10.60	8.35	35.29
T2R1	10.61	8.32	35.51
T2R2	10.59	8.35	35.54

Initial analysis of the spatial correlation characteristics for the proposed model are shown in Figs. 6 and 7. Fig. 6 shows the correlation characteristics in the time domain by calculating the correlation coefficients of two channel impulse responses. As expected, correlation coefficients decrease with increased antenna spacing. Another interesting finding in Fig. 6 is that greater sampling intervals lead to higher correlations. This is echoed by [4] which reports that better channel resolutions lead to greater multiplexing gains. By taking the FFT of the channel impulse response and calculating the correlation coefficients at each frequency point, Fig. 7 shows the frequency correlations against antenna spacing. Smaller correlation coefficients are observed for higher frequencies. This is echoed by measurement results shown in [20]. These two initial analysis indicate that the proposed model is able to yield desirable spatial characteristics. However, we also note that more measurement inputs are needed to further adjust the model parameters and validate its correlation characteristics.

V. CONCLUSION

This paper proposes a correlation based double directional model for indoor MIMO-UWB propagation channels. Differing from conventional CBSMs, we model the channel in the passband and propose to introduce spatial correlations to the amplitude matrices and delay matrices separately. Correspondingly, two correlation matrices are defined explicitly to characterize the correlation properties in both the amplitude and delay domains. The model is implemented based on available parameters and then evaluated by simulations. We validate our model by first showing it to be compatible with the IEEE 802.15.3a standard model. In addition, the initial analysis indicates that the model is able to yield desirable spatial correlation characteristics in both the time and frequency domains.

REFERENCES

- [1] L. Q. Yang and G. B. Giannakis, "Analog space-time coding for multi-antenna ultra-wideband transmissions," *IEEE Trans. on Commun.*, vol. 52, no. 3 pp. 507-517, Mar. 2004.
- [2] L. C. Wang, W. C. Liu, and K. J. Shieh, "On the performance of using multiple transmit and receive antennas in pulse-based ultrawideband systems," *IEEE Trans on Wireless Commun.*, vol. 4, no. 6, pp. 2738-2750, Nov. 2005.
- [3] N. A. Kumar and R. M. Buehrer, "Application of layered space-time processing to ultra wideband communications," *45th Midwest Symposium on Circuits and Systems*, Aug. 2002, pp. 597-600.
- [4] V. P. Tran and A. Sibille, "UWB spatial multiplexing by multiple antennas and RAKE decorrelation," *2nd International Symposium on Wireless Commun. Systems*, Sept. 2005, pp. 272-276.
- [5] T. H. Chang, Y. J. Chang, C. H. Peng, Y. H. Lin and C. Y. Chi, "Space time MSINR-SRAKE receiver with finger assignment strategies in UWB multipath channels", *IEEE International Conf. on Ultra-Wideband*, Sept. 2005, pp. 242-247.
- [6] L. Q. Yang and G. B. Giannakis, "Space-Time Coding for Impulse Radio", *IEEE Conf. on Ultra Wideband Systems and Tech.*, May 2002, pp. 235-239.
- [7] J. Foerster, P802.15-02/490r1-SG3a-Channel-Modeling-Subcommittee-Report-Final.doc, <http://grouper.ieee.org/groups/802/15/pub>.
- [8] D. S. Shiu, G. J. Foschini, M. J. Gans and J. M. Kahn, "Fading correlation and its effect on the capacity of multielement antenna systems," *IEEE Trans Commun.*, vol. 48, no. 3, pp. 502-513, Mar. 2000.
- [9] J. Kunisch and J. Pamp, "Measurement results and modeling aspects for the UWB radio channel," *IEEE Conf. on Ultra Wideband Systems and Tech.*, May 2002, pp. 19-23.
- [10] J. Kunisch and J. Pamp, "An ultra-wideband space-variant multipath indoor radio channel model," *2003 IEEE Conf. on Ultra Wideband Systems and Tech.*, Nov. 2003, pp. 290-294. IEEE.
- [11] L. Schumacher, "Recent advances in propagation characterisation and multiple antenna processing in the 3GPP framework," *Proc. of XXVth URSI General Assembly 2002*, Maastricht, The Netherlands, Aug. 2002.
- [12] A. Saleh and R. A. Valenzuela, "A statistical model for indoor multipath propagation," *IEEE J. Selected Areas Comm.*, vol. 5, no. 2, pp. 137-138, Feb. 1987.
- [13] M. Steinbauer, A. F. Molisch and E. Bonek, "The double-directional radio channel," *IEEE Antennas and Propagation Magazine*, vol. 43, no. 4, pp. 51-63, Aug. 2001.
- [14] J. Karedal, S. Wyne, P. Almers, F. Tufvesson, and A. F. Molisch, "Statistical analysis of the UWB channel in an industrial environment," *Proc. IEEE VTC fall 2004*, 2004, pp. 81-85.
- [15] U. Schuster and H. Bolcskei, "How different are UWB channels from conventional wideband channel?," *IEEE International Workshop on Convergent Technologies*, June 2005, Oulu, Finland.
- [16] L. Schumacher, K. I. Pedersen and P. E. Mogensen, "From antenna spacings to theoretical capacities - guidelines for simulating MIMO systems," *PIMRC 2002*, Sept. 2002, pp. 587-592.
- [17] J. P. Kermaol, L. Schumacher, K. I. Pedersen and P. E. Mogensen, "A stochastic MIMO radio channel model with experimental validation," *IEEE J. on Selective Areas in Commun.*, vol. 20, no. 6, pp. 1211-1226, Aug. 2002.
- [18] D. J. Krus, "Imaging higher transcendental functions in 3-Dimensions," *Journal of Visual Statistics*, vol. 1, pp. 6-9, 2002.
- [19] R. J. M. Cramer, R. A. Scholtz and M. Z. Win, "Evaluation of an ultra-wide-band propagation channel," *IEEE Tran. on Antennas and Propagation*, vol. 50, no. 5, pp. 561-570, May 2002.
- [20] J. S. Liu, B. Allen, W. Q. Malik and D. J. Edwards, "A measurement based spatial correlation analysis for MB-OFDM ultra wideband transmissions," *Loughborough Antenna and Propagation Conf.*, Apr. 2005, UK.

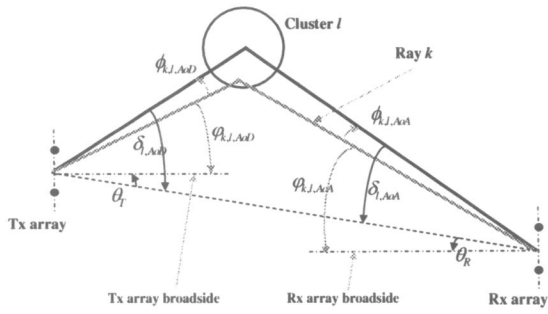


Fig. 1. Relationships of angles.

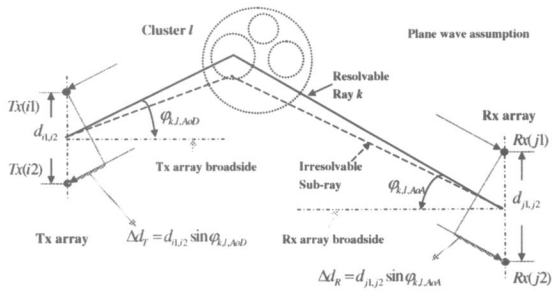


Fig. 2. IAPD in a 2×2 MIMO link.

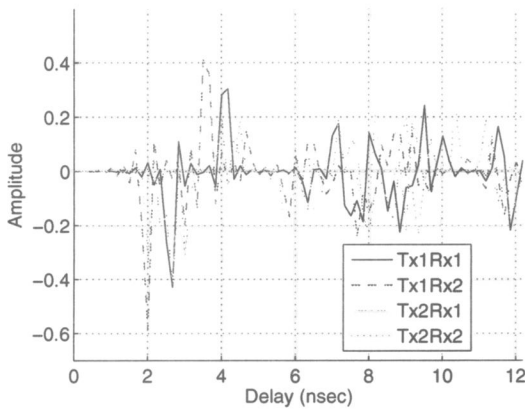


Fig. 3. Example realization of a 2×2 MIMO channel (CM2, $d_T = 10$ cm, $d_R = 20$ cm and $T_s = 0.167$ ns).

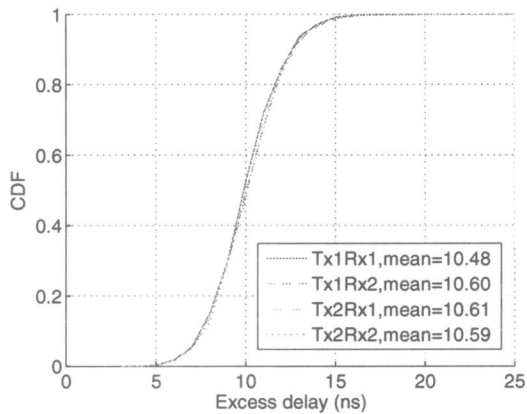


Fig. 4. CDF of channel excess delays (CM2, $d_T = 10$ cm, $d_R = 20$ cm and $T_s = 0.167$ ns).

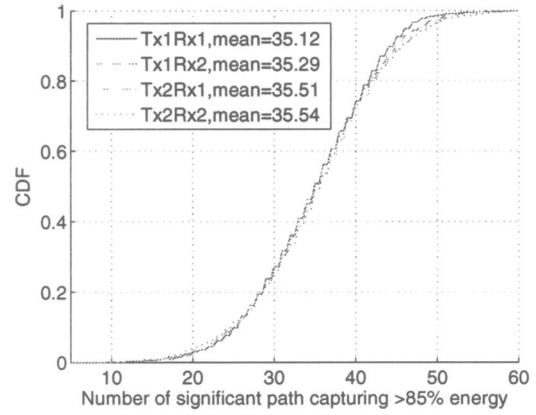


Fig. 5. CDF of the number of significant paths that capture 85 percent of the channel energy (CM2, $d_T = 10$ cm, $d_R = 20$ cm and $T_s = 0.167$ ns).

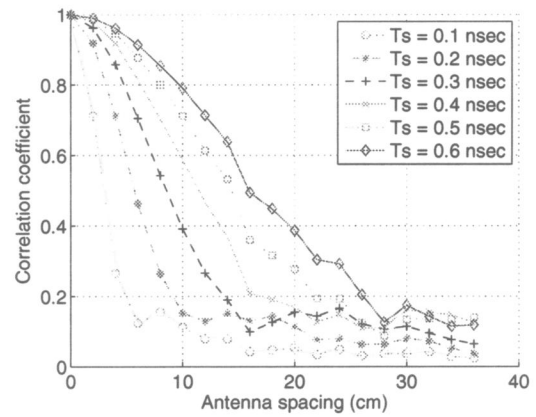


Fig. 6. Channel impulse response correlation against antenna spacing and sampling interval (CM2, $d_T = 0$).

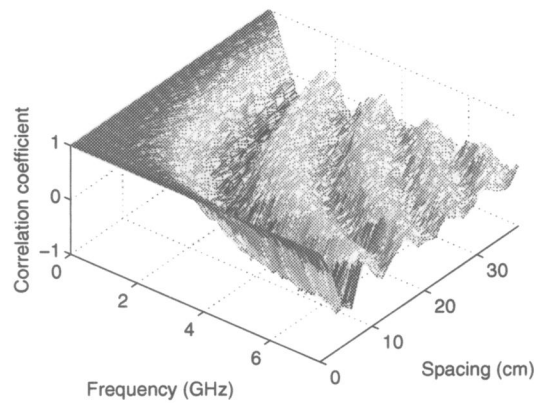


Fig. 7. Frequency correlation (CM2, $d_T = 0$ and $T_s = 0.133$ ns).